Accepted Manuscript

Title: Competitive adsorption, selectivity and separation of valuable hydroxytyrosol and toxic phenol from olive mill wastewater

Authors: Asma Yangui, Jacques Romain Njimou, Agnese Cicci, Marco Bravi, Manef Abderrabba, Angelo Chianese

PII: S2213-3437(17)30288-9
DOI: http://dx.doi.org/doi:10.1016/j.jece.2017.06.037
Reference: JECE 1699

To appear in:

Received date: 11-4-2017
Revised date: 17-6-2017
Accepted date: 19-6-2017

Please cite this article as: Asma Yangui, Jacques Romain Njimou, Agnese Cicci, Marco Bravi, Manef Abderrabba, Angelo Chianese, Competitive adsorption, selectivity and separation of valuable hydroxytyrosol and toxic phenol from olive mill wastewater, Journal of Environmental Chemical Engineeringhttp://dx.doi.org/10.1016/j.jece.2017.06.037

Competitive adsorption, selectivity and separation of valuable hydroxytyrosol and toxic phenol from olive mill wastewater

Asma Yangui[a,b,*], Jacques Romain Njimou[c], Agnese Cicci[c], Marco Bravi[c], Manef Abderrabba[a], Angelo Chianese[c]

[a] Preparatory Institute for Scientific and Technical Studies (IPEST), Laboratory of Materials, Molecules and Applications (LMMA), BP 51 La Marsa 2070, Tunisia

[b] University of Tunis El Manar, Faculty of Sciences of Tunis, Campus University 2092, El Manar, Tunis, Tunisia

[c] Department of Chemical Engineering, University of Rome ‘‘La Sapienza’’, Via Eudossiana, 18-00184 Rome, Italy

* Corresponding author.

Tel: 00216 23 455 367.

E-mail address: yangui.asma@gmail.com

Graphical abstract

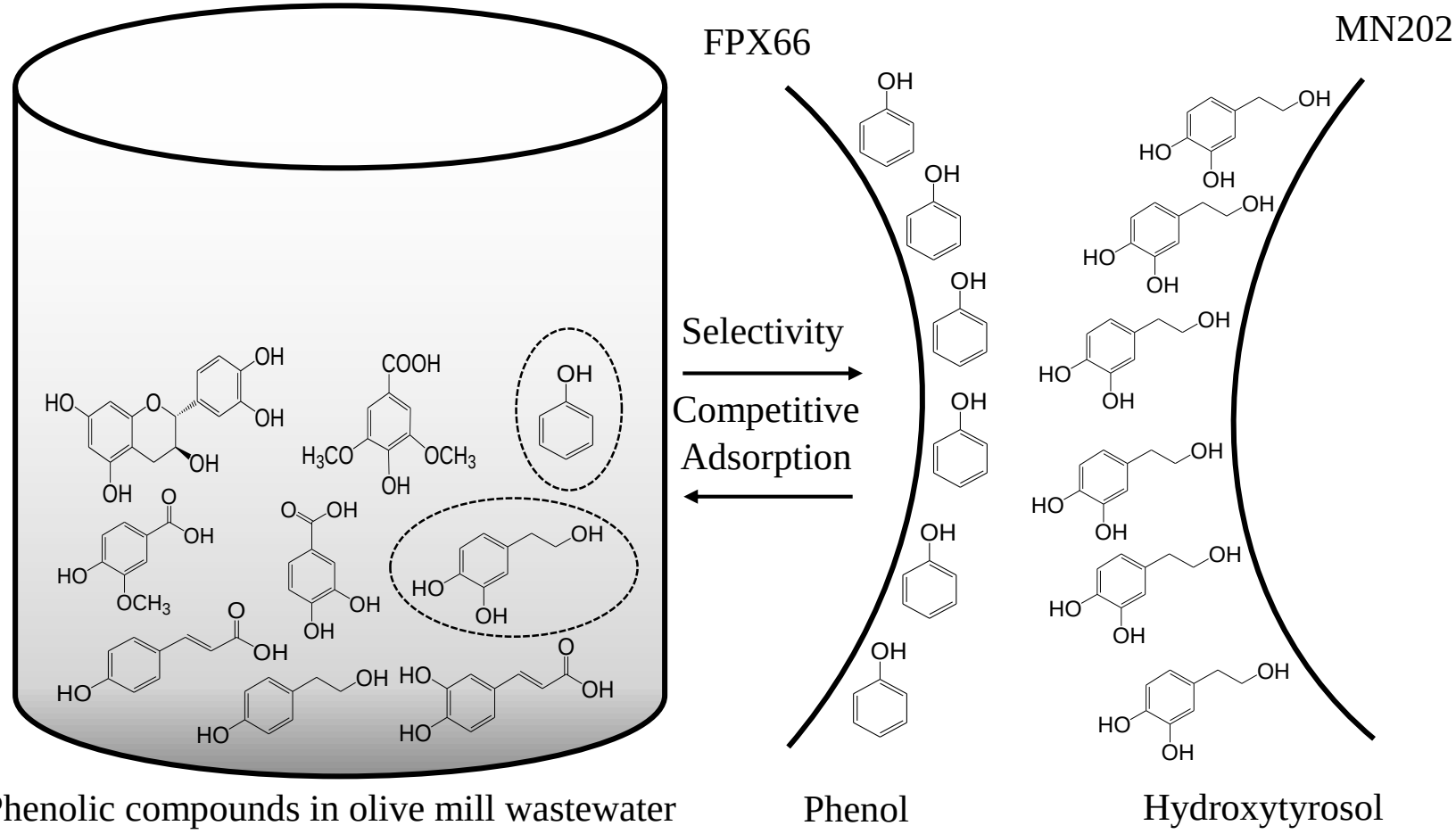

Highlights

- The competitive adsorption of a large number of phenolic compounds was assessed from olive mill wastewater.
- Higher selectivity coefficient for phenol over hydroxytyrosol was displayed on FPX66.
- The adsorption and the recovery percentage of hydroxytyrosol on MN202 was greater than 91 %.
- FPX66 was exhibited a multilayer adsorption characteristic, whereas a monolayer adsorption was attributed to MN202.

Abstract

Competitive adsorption and selectivity of toxic phenol and hydroxytyrosol were studied on the macroreticular aromatic polymer (FPX66) and the macroporous polystyrene cross linked with divinylbenzene (MN202). The adsorption equilibrium of phenol and hydroxytyrosol as well as other phenolic compounds in olive mill wastewater (OMW) was investigated taking into account the different affinities of these compounds towards the two above mentioned resins. The experimental results showed that the adsorption equilibrium of phenol on FPX66 can be well interpreted by the BET model, indicating a multilayer adsorption, whereas, the adsorption of hydroxytyrosol on MN202 at equilibrium is well fitted by the Sips model. At low FPX66 concentration, phenol exhibited much higher adsorption percentage than hydroxytyrosol, indicating a stronger interaction with the resin. The adsorption selectivity ratio of phenol/ hydroxytyrosol was of about 3.215 at 5 g L^{-1} of FPX66. Thanks to the large affinity of hydroxytyrosol for the MN202 resin, its adsorption and recovery were higher than 90% on this resin. Thus, under suitable operating conditions, phenol was selectively separated on FPX66, while hydroxytyrosol was largely recovered from the OMW residual solution by adsorption on MN202.

Keywords: Competitive adsorption; Selectivity; Separation; Hydroxytyrosol; Phenol; Equilibrium models

1. Introduction

The olive oil extraction system consists of three operational steps including the olives crushing, the malaxation of the resulting paste and the separation of olive oil from the remaining wastewater, named olive mill wastewater (OMW). This latter essentially consists of water added during the malaxation step of olive fruits, the olives water content and the residual oil after the centrifugation step. Its amount is about 30 million m^3 per year [1].

OMW is characterized by high concentrations of organic compounds (40-220 g L^{-1}) [2], which inhibit the natural degradation of the wastewater. This liquid waste is often used for irrigation as fertilizer [3]. Nonetheless, high concentrations of phenolic compounds may not only inhibit the germination of plant seeds but infiltrate through soil layers and contaminate the ground water [4]. Otherwise, chemical - physical and biological methods such as precipitation, flocculation, coagulation, and filtration were proposed, but they give only incomplete solution to the problem. Other methods like reverse osmosis and ultrafiltration were successfully investigated, however its high cost cannot be ignored [5]. Research studies have proved that the real treatment of OMW cannot been achieved without combinations of existing technologies [6]. Hence, OMW must be treated by removing most of its organic charge, especially phenolic compounds. However, several antioxidants, denoted polyphenols with proven health benefits [7-9] are present in OMW such as hydroxytyrosol, 3,4-dihydroxybenzoic acid, tyrosol, caffeic acid, vanillic acid, catechin, syringic acid, p-coumaric acid, etc. Among the above mentioned phenolic compounds in OMW, hydroxytyrosol is the most representative active compound and exhibits relevant properties such as strong antioxidant, anti-inflammatory, antiatherogenic and antiplatelet, antiproliferative and anti-cancer activities [10,11]. It has to be noticed that, before the extraction of hydroxytyrosol, molecular phenol, sometime present in significant amounts in OMW, must be removed [12].

The phenol adsorption avoids its hazardous release into the environment [13,14]. Consequently, an OMW treatment with the removal of toxic phenol and the recovery of valuable hydroxytyrosol are of great interest, both economically and environmentally. It is well known that adsorption is an effective technique which requires relatively low economic investment, quite high energy saving and high efficiency in removal, recovery and selective separation of some compounds. In the recent years, several studies dealt with the uptake of polyphenols and other bioactive compounds from OMW on different adsorbents [15-19]. Several polymeric resins have attracted increasing attention due to their high adsorption capacities towards phenolic compounds from OMW. For example, XAD16 and XAD7HP resins were used as efficient adsorbents for polyphenol and hydroxytyrosol

for environmental remediation of OMW [20]. XAD7, XAD16, IRA96 and the Isolute ENV+ resins showed good adsorption for low molecular weight polyphenols from OMW [21].

The previous authors were focused only and mainly on polyphenols recovery from OMW such as hydroxytyrosol. However, no reports concerned the selective separation of toxic phenol and hydroxytyrosol from OMW. The main aim of this study is the investigation on the selective removal of toxic phenol and the recovery of phenol-free extract containing pure hydroxytyrosol, by taking into account the different affinities of these two compounds towards two absorbent resins with different characteristics, which are FPX66 and MN202. The choice of these two resins is in fact based on their different adsorption capacity with respect to phenol and hydroxytyrosol, respectively. FPX66 adsorbs better non-polar molecules as phenol, whereas MN202 adsorbs better polar molecule as hydroxytyrosol.

2. Materials and methods

2.1. Materials

The olive mill wastewater was collected from an oil mill factory near Rome. It was centrifuged to eliminate the solid residue of the olive oil extraction process. A centrifuge Avanti J-20XP, provided of cylindrical burettes, was used for two hours at a constant speed of 7500 rpm and at 22°C. The supernatant liquid phase was collected for the rest of the experiments. The solid residue at the bottom of each burette was approximately estimated 1 g L^{-1}.

Amberlite FPX66 and Purolite MN202 resins were supplied by Dow Chemical company and Purolite Corporation, respectively. Hydroxytyrosol (98%), catechin hydrate (98%), caffeic Acid (99%), syringic acid (95%) and phenol (99%) were all acquired from Sigma Aldrich, whereas tyrosol (99.5%), 3,4-dihydroxybenzoic acid (97%), vanillic Acid (97%) and p-coumaric acid (98%) were were obtained from Fluka. All these standards were of HPLC grade. Higher molecular weight polyphenols are normally present in much lower amounts in OMW because they have undergone natural or artificial hydrolysis to lower molecular weight polyphenols (e.g. oleuropein to hydroxytyrosol) [22]. For this reason, they were not separately considered in this study.

Potassium dichromate (99%) reagent was procured by Sigma-Aldrich, silver sulfate solution and mercury (II) sulfate (99%) reagent were supplied by Fluka and used for the COD determination. The following analytical grade solvents were used: acetonitrile (HPLC grade) by J.T Baker and ethanol 99.8% by Fluka. Bi-distilled water was used for resin pretreatment and for HPLC analysis.

2.2. Characterisation

2.2.1. *Characterisation of feedstock and recovered materials*

Purolite MN202 resin is a macroporous polystyrene cross linked with divinylbenzene (surface area of 825 m^2 g^{-1}, mean diameter of 585 ± 85 μm and pore volume of 1.0 – 1.1 mL g^{-1}) [Hypersol-Macronet® MN202, product data sheet August 2015]. This resin is very suitable for an efficient sorption of high molecular organic molecules and is easily regenerated. FPX66 is a non-ionic macroreticular aromatic polymer non-functionalized resin (surface area of 700 m^2 g^{-1}, harmonic mean size 600 – 750 μm and pore volume of 1.4 mL g^{-1}) [AmberliteTM FPX66, ROHM and HAAS data sheet, apr. 2008]. This resin preferentially adsorbs non-polar molecules over hydrophobic interactions, while polar molecules are retained less strongly [23]. Both resins were chosen because of their different affinities towards polar and non-polar molecules in OMW and their simple pretreatment and chemical regeneration characteristics.

Activations of the resins were carried as follows: FPX66 and MN202 were immersed in bi-distilled water and were purged in a vacuum system. Then, they were filtered by Buchner filter connected to a vacuum pump system. The resins were collected in separate beakers. Ethanol was then added under stirrer (120 rpm) for two hours. Subsequently, the resins were recovered

by filtration, washed and dried. In order to examine which functional groups were responsible for the adsorption of phenolic compounds, ATR-FTIR spectroscopy analysis of MN202 and FPX66 after ethanol activation was carried.

2.2.2. *Characterisation of aqueous samples*

Quantitative measurements of different phenolic compounds in OWM were performed on HPLC instrument (Agilent 1200) using C18 column (4.6 mm × 250 mm, 5 μm i.d., Teknokroma) at a fixed temperature of 20 °C. The separation was achieved in gradient mode using acetic acid in bi-distilled water 0.5% (A) and acetonitrile (B). The eluent composition-initially equal to 100% (A), was changed gradually to 55% (A) and 45% (B) in 45 min, then again gradually to the initial solvent composition to the end of the run. The analysis time was set at 60 min, the eluent flow rate was 1.0 mL min^{-1} and the detection wavelength was set at 280 nm.

The composition of phenolic compounds in OMW was based on the peak area of standards. This technique allowed excellent concentration measurements since the linear correlation coefficients (R^2) between predicted and real values was higher than 0.99.

Total phenolic compounds content was measured at a wavelength of 280 nm [17] using syringic acid as an analytical standard, whereas the color removal was measured at a wavelength of 395 nm on UV-Vis spectrophotometer [17, 24].

Chemical oxygen demand (COD) was measured by photometric determination of the chromium (III) concentration after 2 h of oxidation with potassium dichromate solution mixed with silver sulfate in sulfuric acid solution at 148 ± 2°C (German standard methods DIN 38 409-H41-1 and DIN ISO 15 705-H45) [25].

The main characteristics of OMW are reported in Table 1. The names, the chemical structures and the concentrations of phenolic compounds are shown in Fig. 1.

Table 1

Fig. 1

Adsorption equilibrium experiments were carried out by mixing a fixed volume of OMW with a fixed mass of the examined resins for 24 h. The mixing equipment was a shaking incubator operated at a fixed speed of 150 rpm. The adsorption equilibrium parameters were determined at resin concentrations in the range between 5 and 100 g L^{-1}. The adsorption capacity at equilibrium conditions, q_e (mg g^{-1}), was calculated by Eq. (1).

$$q_e = \frac{(C_0 - C_{eq})}{X} V \quad (1)$$

where, V is the OMW volume (L), x is the mass of the adsorbent (g) and C_0 and C_{eq} are the initial and the equilibrium concentrations (mg L^{-1}), respectively.

The fitting of the experimental adsorption data set was attempted by using Langmuir, Freundlich, Sips, Redlich-Peterson and BET equilibrium isotherm equations [26,27]. The error analysis was achieved by estimating the normalized deviation (ND) and the normalized standard deviations (NSD) using Eqs. (2) and (3) [28].

$$ND = \frac{100}{n} \sum \left| \frac{q_{e(exp)} - q_{e(pred)}}{q_{e(exp)}} \right| \quad (2)$$

$$NSD = 100 \sqrt{\frac{\sum ((q_{e(exp)} - q_{e(pred)})/q_{e(exp)})^2}{n}} \quad (3)$$

Where, $q_{e(exp)}$ and $q_{e(pred)}$ are the experimental and predicted adsorption capacities (mg g^{-1}), respectively, and n is the number of observations.

Desorption experiments were carried out on the resins recovered by filtration using ethanol with or without HCl 0.1 M. After desorption, the materials were rinsed with bidistilled water and were re-

used to check the efficiency of their recycling. Three cycles of adsorption-desorption-regeneration were usually accomplished.

The adsorption efficiencies (R_{Phenol} %), (R_{Color} %) and (R_{COD} %) were calculated using Eq. (4), (5) and (6).

$$R_{Phenol} = \frac{C_0 - C_F}{C_0} \times 100 \quad (4)$$

where C_0 (mg L^{-1}) and C_F (mg L^{-1}) are the initial and the final concentrations of total phenols.

$$R_{Color} = \frac{Abs395_0 - Abs395_F}{Abs395_0} \times 100 \quad (5)$$

where $Abs395_0$ (nm) and $Abs395_F$ (nm) are the absorbance of OMW at 395 nm before and after treatment.

$$R_{COD} = \frac{COD_0 - COD_F}{COD_0} \times 100 \quad (6)$$

where COD_0 (g L^{-1}) and COD_F (g L^{-1}) are the initial and the final values of the chemical oxygen demand, respectively.

3. Results and discussions

3.1. Structural characteristics of the resins

Attenuated total reflectance Fourier transform infrared (ATR-FTIR) spectra were recorded for both resins (Fig. 2). A large band centered at 3440 cm^{-1} attributed to adsorbed H_2O molecules was observed only for the MN202 resin. The bands at 3020−2800 cm^{-1} attributed to aromatic stretching vibrations and to the aliphatic C−H groups, were also observed. The adsorption bands between 1604 and 1430 cm^{-1} were assigned to aromatic C=C bonds. The bands at 1315 and 1037 cm^{-1} were associated with phenol groups and the band at 1160 cm^{-1} was assigned to aromatic C-H deformation of CH_3 [29,30]. The bands at 910−740 cm^{-1} were attributed to the deformation of C−H bond in the benzene rings. The band at 1671 cm^{-1} and the shoulder at 1604 cm^{-1} were assigned to C=C stretching vibration [30].

Fig. 2

3.2. Adsorption studies

The removal of total phenols (a) and color from OMW sample onto MN202 and FPX66 are shown in Fig. 3. When the resin concentration increases, the adsorption removal increases as well, as expected, and a higher percentage of phenolic compounds is removed up to an apparent plat point,

which is attained at steady state. The fast increase in the adsorption percentage occurring at higher adsorbent concentration up to 20 g L^{-1} is attributed to the availability of more actives sites [17]. At smaller resins concentrations, less than 20 g L^{-1}, FPX66 is more effective, whereas as well as the resin concentration rises, MN202 becomes more efficient for the removal of both the color and the total phenols. The best results obtained using MN202 were 84% color removal and 88% total phenols reduction. Therefore, the adsorption percentages of MN202 is more effective than zeolite, which showed adsorption percentages of 24.7% and 77% for total phenols and dark color of OMW [24].

Fig. 3

MN202 exhibited higher maximum adsorption capacity of total phenols (175.1 mg g^{-1}) compared to FPX66 (102.3 mg g^{-1}). The novel resins seem to be more effective than some adsorbents reported in the literature for similar application. Santi et al. [15] revealed a maximum adsorption capacity of 11.4 mg g^{-1} using incompletely combusted olive pomace as adsorbent. Martino et al. [16] measured maximum adsorption capacities only of 46.7 mg g^{-1}, 69 mg g^{-1}, 15.7 mg g^{-1} and 10.2 mg g^{-1} onto layered double hydroxide of magnesium and aluminium (LDH), LDH after calcination at 450°C (LDH-450), hydroxyaluminium–iron–co–precipitate (HyAlFe) and hydroxy–aluminium–iron–montmorillonite comple (HyAlFe-Mt), respectively. In conclusion either FPX66 or MN202 showed better results for the adsorption capacities compared the above-mentioned work, moreover MN202 showed the best performances in terms of percentage of color and total phenols removal with respect to the literature works.

3.3. Selectivity

A wide experimental plan was worked out and a high selectivity coefficient of hydroxytyrosol over phenol was achieved onto MN202 and vice versa onto FPX66. The results showed that it was feasible to efficiently separate hydroxytyrosol and phenol using FPX66 resin and largely recover hydroxytyrosol using MN202 resin from OMW.

The adsorption data of the two resins with respect to each phenolic compound are quantitatively compared in terms of the adsorption percentage using two different concentrations of both resins (5 g L^{-1} and 50 g L^{-1}), which are the smallest and the average concentrations used in the current work. The selectivity coefficient (K) with respect to tyrosol was also determined as the ratio between adsorption percentages between each phenolic compound and tyrosol [31].

Apparently, there is a good correlation between adsorption percentages resulted from HPLC studies (Table 2) and from the total phenols measurements on UV spectrophotometer (Fig. 3a). In fact, when the resin concentration increases, MN202 exhibited higher adsorption percentage whereas, at lower resin concentration, FPX66 showed better results.

Table 2

It should be noticed that the selectivity of hydroxytyrosol is the smallest among all the examined phenols: 0.307 onto FPX66 at low resin concentration (5 g L^{-1}). It increases only to 0.601 for a FPX66 resin concentration of 50 g L^{-1}. The most significant adsorption percentages obtained on FPX66 at 5 g L^{-1} were reached for tyrosol and phenol. Therefore, we may conclude that phenol was quite easily and effectively adsorbed on FPX66 resin. From the above results, phenol was selectively adsorbed and separated onto FPX66 while hydroxytyrosol remains in the residual solution. Meanwhile, the selectivity of hydroxytyrosol on MN202 is high, reaching a selectivity coefficient value of 0.920 at the average mass of the resin (50 g L^{-1}).

These results were also confirmed by the ratio between the selectivity of phenol and that one of hydroxytyrosol on FPX66 (5 g L^{-1}), which was significantly high, that is equal to 3.215. Thus, it is believed that FPX66 is appropriate to capture toxic phenol from OMW under the condition of 5 g L^{-1} and only slightly adsorbs hydroxytyrosol, which is the most sought after component. The forgoing data indicate that the separation between phenol and hydroxytyrosol from real olive mill wastewater could be accomplished on FPX66.

For the effective separation of toxic phenol and the recovery of hydroxytyrosol, the primary stage on FPX66 (5 g L^{-1}) is required to selectively adsorb phenol. The resulting aqueous solution, containing hydroxytyrosol concentration of 603.95 mg L^{-1}, was then used as the feeding solution of the second stage on MN202 (50 g L^{-1}). Subsequently, a complete adsorption of hydroxytyrosol was achieved.

3.4. Adsorption isotherms

The adsorption experimental data were interpreted using some equilibrium models and the best equilibrium parameters were determined. The fitting of the isotherms experimental data has been attempted using all the most used equilibrium models: Langmuir, Freundlich, SIPS, Riedlich-Peterson and BET, in particular all such models were used to fit the adsorption data on FPX66, whereas all the models except BET isotherm on MN202 equilibrium data. At first glance,

equilibrium curves on FPX66 and MN202 seem to be of types III and I, respectively (Fig. 4 and 5).

Fig. 4

Fig. 5

The best fitting parameters and regression coefficients are reported in Table 3 and 4. It is interesting to notice that the values of the parameter "n" of the Freundlich equation, calculated for all solutes adsorption, were in the range between 0 and 10, indicating that the adsorption onto both FPX66 and MN202 resins was favorite at the studied conditions [32]. The values of the regression coefficients, the normalized deviation ND and the normalized standard deviation NSD indicate that the best fitting of the adsorption data on MN202 are provided by the Sips equation, which is derived from the limiting behavior of the Langmuir and Freundlich isotherms. Since this model is valid for localized adsorption without adsorbate-adsorbate interactions [33], it is possible to consider that the effect of the different adsorbates, contemporary present over the resin surface is negligible. On the contrary, the FPX66 isotherms curves in Fig. 4, exhibiting an exponential increase of the adsorbed compounds, show a typical III adsorption behavior. The same type of adsorption was observed by Bertin et al. [21] for hydroxytyrosol adsorption on XAD7, XAD16, IRA96 and ENV+ resins.

Table 4

Table 5

By comparing the quality of the experimental data fitting on the basis of the values of the regression coefficient R^2, the normalized deviation ND and the normalized standard deviation NSD, it can be seen that the BET model provides the best fit for FPX66 resin. This isotherm presents better fitting on microporous or mesoporous adsorbents and is convex at higher relative concentration. It is favored by weak interaction between adsorbate-adsorbent system and strong interaction between the adsorbate molecules, leading to the multilayer formation [34]. In fact, the interaction occurring between the adsorbate and the first adsorbed layer is higher than the interaction with the material surface [35]. This adsorption behavior suggests that intraparticle diffusion within the pores does not occur [36]. This result is consistent with data reported by Nassar et al. [37], which indicate that BET model gives the best fit of the adsorption of phenolic compounds from OMW using magnetic nanoparticles [37].

3.5. Adsorption mechanism

The adsorption interaction mechanism on both adsorbents may be interpreted on the basis of the different adsorption characteristics of the resins, as the structural parameters including the surface area, the pore volume, the pore size, and the functional groups on the adsorbent surface [38, 39]. On the one hand, total phenols and color removal adsorption is more effective on MN202, which could be explained by the higher surface area of MN202 (850 m^2 g^{-1}) compared to FPX66 (700 m^2 g^{-1}). On the other hand, the functional groups over the adsorbent surface determines polarity of the resins, so playing an important role in the adsorption process. Polar materials adsorb polar substrates [40]. FPX66 is a non-functionalized adsorbent, thus it better adsorbs non-polar molecules due to hydrophobic interactions, while polar molecules are less strongly retained. Hence, the highest uptake of phenol and the lowest uptake of hydroxytyrosol are justified on the light of pour polarity of phenol and the high polarity of hydroxytyrosol. Both compounds are acids and their numbers of OH-functional groups (one for phenol and three for hydroxytyrosol) may determine their polarity and accordingly their affinity with respect to the resins. At the same time, the polarity of MN202 can explain the highest uptake of hydroxytyrosol on MN202 compared to FPX66 at the same experimental conditions. The polarity matching between MN202 and hydroxytyrosol is mostly attributed to multiple adsorption interactions as follows [41,42]. On the one hand, MN202 is aromatic, thus, the adsorption takes place through π–π interactions. On the other hand, the adsorption process depends mainly on two influencing factors which are: the phenolic ionized species in the solution and the overall charge of the adsorbent. The overall charge of MN202 derives from the protonation and the deprotonation of the benzene ring. The medium of the adsorption process is acidic (pH = 4.2), hence, hydroxytyrosol remains in its undissociated form (pH<pKa) and the surface of MN202 becomes positively charged, which can enhance the ion–dipole interactions with the polar adsorbate.

Compared to MN202, FPX66 adsorbs non-polar phenolic compounds, which may explain the highest adsorption rate of phenol compared to hydroxytyrosol. In fact, the adsorption percentage on FPX66 decreases with the enhancement of the polarity of the adsorbate (Table 2).

3.6. Desorption and regeneration studies

In general, the solvent desorption efficiency on both resins depends on the specific compound and the extraction solvent. The desorption of phenolic compounds from FPX66 and MN202 resins using ethanol and acidified ethanol (0.1 M HCl in ethanol) was studied. The obtained experimental data are reported in Fig. 6.

Fig. 6

We may observe that the desorption is always higher than 90 % on both resins and easier on MN202 than on FPX66. The desorption percentage on MN202 is always quantitative using ethanol, however, employment of acidified ethanol gave rise to improved desorption efficiency on FPX66. This is in complete agreement with a previous study dealing with the desorption of phenolic compounds from OMW on Amberlite resins [21].

Because of the small difference of the desorption percentages using ethanol or acidified ethanol, the first solvent must be selected as eco-friendly desorbing medium.

After the desorption of phenolic compounds, the resins were washed with bidistilled water, dried and reused again for new adsorption cycles. The adsorption percentages of phenolic compounds were the same after resins treatments. Thus, the structures of the adsorbents were not modified during the whole adsorption-desorption process. No significant changes in the adsorption capacity were observed over three cycles, indicating that ethanol treatment helps to keep the pores actives and that both adsorbents were successfully regenerated.

4. Conclusion

The two examined resins, i.e. FPX66 and MN202, exhibited different adsorption characteristics with respect to the phenolic components of the used OMW. The adsorption on FPX66 has a multilayer characteristic, whereas a monolayer adsorption model is predominant for the adsorption on MN202. The adsorption process occurring at a low concentration of FPX66 allows the selective removal of phenol. On the contrary, if MN202 is used a quantitative adsorption of MN202 takes place. Therefore, this work was expected to provide some understandings into the selective separation of toxic phenol molecule from OMW and to develop an effective recovery of hydroxytyrosol. The polarity of both the adsorbate and the adsorbent was confirmed to be the key factor for the interpretation of the separation results.

Acknowledgments

The Authors acknowledge the financial supports received from the Department of Chemical Material Environmental Engineering, Sapienza University of Rome, the Laboratory of Materials Molecules and Applications, Preparatory Institute for Scientific and Technical Studies, University of Carthage, and the Department of Chemistry, University of Tunis El Manar.

References

[1] E.S. Aktas, S. Imre, L. Ersoy, Characterization and lime treatment of olive mill wastewater, Water Res. 35 (2001) 2336–2340.

[2] I. Ntaikou, C. Kourmentza, E.C. Koutrouli, K. Stamatelatou, A. Zampraka, M. Kornaros, G. Lyberatos, Exploitation of olive oil mill wastewater for combined biohydrogen and biopolymers production, Bioresour. Technol. 100 (2009) 3724–3730.

[3] R. Altieri, A. Esposito, Olive orchard amended with two experimental olive mill wastes mixtures: effects on soil organic carbon, plant growth and yield, Bioresour. Technol. 99 (2008) 8390–8393.

[4] R. Jarboui, F. Sellami, A. Kharroubi, N. Gharsallah, E. Ammar, Olive mill wastewater stabilization in open air ponds: impact on clay–sandy soil, Bioresour. Technol. 99 (2008) 7699–7708.

[5] S. Azabou, W. Najjar, A. Gargoubi, A. Ghorbel, S. Sayadi, Catalytic wet peroxide photo-oxidation of phenolic olive oil mill wastewater contaminants Part II. Degradation and detoxification of low-molecular mass phenolic compounds in model and real effluent, Appl. Catal. B. 77 (2007) 166–174.

[6] P. Paraskeva, E. Diamadopoulos, Technologies for olive mill wastewater (OMW) treatment: a review, J. Chem. Technol. Biotechnol. 81 (2006) 1475–1485.

[7] F. Ferri, L. Bertin, A. Scoma, L. Marchetti, F. Fava, Recovery of low molecular weight phenols through solid-phase extraction, Chem. Eng. J. 166 (2011) 994–1001.

[8] B. Bassani, T. Rossi, D.D. Stefano, D. Pizzichini, P. Corradino, N. Macrì, D.M. Noonan, A. Albini, A. Bruno, Potential chemopreventive activities of a polyphenol rich purified extract from olive mill wastewater on colon cancer cells, J. Funct. Foods 27 (2016) 236–248.

[9] F. Hajji, B. Kunz, J. Weissbrodt, Polymer incompatibility as a potential tool for polyphenol recovery from olive mill wastewater, Food Chem. 156 (2014) 23–28.

[10] M.C. Ramírez-Tortose, M. Pulido-Moran, S. Granados, J.J. Gaforio, J.L. Quiles, Hydroxytyrosol as a component of the mediterranean diet and its role in disease prevention, in: V.R. Preedy, R.R. Watson, editors, The mediterranean diet (an evidence-based approach), Elsevier Inc., United States of America, 2015, pp. 205 – 215.

[11] P. Ramosa, S.A.O. Santos, Â.R. Guerraa, O. Guerreiroa, L. Felício, E. Jerónimo, A.J.D. Silvestre, C.P. Neto, M. Duarte, Valorization of olive mill residues: Antioxidant and breast cancer antiproliferative activities of hydroxytyrosol-rich extracts derived from olive oil by-products, Ind. Crop. Prod. 46 (2013) 359–368.

[12] A. Cicci, M. Stoller, M. Bravi, Microalgal biomass production by using ultra- and nanofiltration membrane fractions of olive mill wastewater, Water Res. 47 (2013) 4710–4718.

[13] J. Huang, K. Huang, S. Liu, Q. Luo, S. Shi, Synthesis, characterization, and adsorption behavior of aniline modified polystyrene resin for phenol in hexane and in aqueous solution, J. Colloid Interf. Sci. 317 (2008) 434–441.

[14] D. Raghu, H. Hsieh, Considerations in disposal of phenolic waters, Inter. J. Environ. Stud. 30 (1987) 277–285.

[15] C.A. Santi, S. Cortes, L.P. D'Acqui, E. Sparvoli, B. Pushparaj, Reduction of organic pollutants in Olive Mill Wastewater by using different mineral substrates as adsorbents, Bioresour. Technol. 99 (2008) 1945–1951.

[16] A.D. Martino, M. Iorio, P.D. Prenzler, D. Ryan, H.K. Obied, M. Arienzo, Adsorption of phenols from olive oil waste waters on layered double hydroxide, hydroxyaluminium–iron-co-precipitate and hydroxyaluminium–iron–montmorillonite complex, Appl. Clay Sci. 80–81 (2013) 154–161.

[17] A. Yangui, M. Abderrabba, A. Sayari, Amine-modified mesoporous silica for quantitative adsorption and release of hydroxytyrosol and other phenolic compounds from olive mill wastewater, J. Taiwan Institute Chem. Eng. 70 (2017) 111–118.

[18] A. Ena, C. Pintucci, P. Carlozzi, The recovery of polyphenols from olive mill waste using two adsorbing vegetable matrices, J. biotechnol. 157 (2012) 573–577.

[19] D.P. Zagklis, A.I. Vavouraki, M.E. Kornaros, C.A. Paraskeva, Purification of olive mill wastewater phenols through membrane filtration and resin adsorption/desorption, J. Hazard. Mater. 285 (2015) 69–76.

[20] A. Agalias, P. Magiatis, A.L. Skaltsounis, E. Mikros, A. Tsarbopoulos, E. Gikas, I. Spanos, T. Manios, A new process for the management of olive oil mill waste water and recovery of natural antioxidants, J. Agric. Food Chem. 55 (2007) 2671–2676.

[21] L. Bertin, F. Ferri, A. Scoma, L. Marchetti, F. Fava, Recovery of high added value natural polyphenols from actual olive mill wastewater through solid phase extraction, Chem. Eng. J. 171

(2011) 1287–1293.

[22] A. Cardinali, S. Pati, F. Minervini, I. D'Antuono, V. Linsalata, V. Lattanzio, Verbascoside, Isoverbascoside, and Their Derivatives Recovered from Olive Mill Wastewater as Possible Food Antioxidants, J. Agric. Food Chem. 60 (2012) 1822–1829.

[23] M. Monsanto, R. Mestrom, E. Zondervan, P. Bongers, J. Meuldijk, Solvent Swing Adsorption for the Recovery of Polyphenols from Black Tea, Ind. Eng. Chem. Res. 54 (2015) 434–442.

[24] G. Padovani, C. Pintucci, P. Carlozzi, Dephenolization of stored olive-mill wastewater, using four different adsorbing matrices to attain a low-cost feedstock for hydrogen photo-production, Bioresour Technol. 138 (2013) 172–179.

[25] A.E. Greenberg, L.S. Clesceri, A.D. Eaton, Standard Methods for the Examination of Water and Wastewater, APHA/AWWA/WEF, 16th ed. Cabs, Washington, DC, 1992.

[26] E. Da'na, A. Sayari, Adsorption of copper on amine-functionalized SBA-15 prepared by co-condensation: Equilibrium properties, Chem. Eng. J. 166 (2011) 445–453.

[27] C.A. Franco, N.N. Nassar, F.B. Cortés, Removal of oil from oil-in-saltwater emulsions by adsorption onto nano-alumina functionalized with petroleum vacuum residue, J Colloid Interf. Sci. 433 (2014) 58–67.

[28] P. Simha, A. Yadav, D. Pinjari, A.B. Pandit, On the behaviour, mechanistic modelling and interaction of biochar and crop fertilizers in aqueous solutions, Resour. -Efficient Technol. 2 (2016) 133–142.

[29] A. Li, Q. Zhang, G. Zhang, J. Chen, Z. Fei, F. Liu, Adsorption of phenolic compounds from aqueous solutions by a water-compatible hypercrosslinked polymeric adsorbent, Chemosphere 47 (2002) 981–989.

[30] M. Özacar, İ.A. Şengil, H. Türkmenler, Equilibrium and kinetic data, and adsorption mechanism for adsorption of lead onto valonia tannin resin, Chem. Eng. J. 143 (2008) 32–42.

[31] C. Micheau, A. Schneider, L. Girard, Evaluation of ion separation coefficients by foam flotation using a carboxylate surfactant, Colloid. Surfaces A: Physicochemical Eng. Aspects 470 (2015) 52–59.

[32] P. Barkakati, A. Begum, M.L. Das, P.G. Rao, Adsorptive separation of Ginsenoside from aqueous solution by polymeric resins: Equilibrium, kinetic and thermodynamic studies, Chem. Eng. J. 161 (2010) 34–45.

[33] K.Y. Foo, B.H. Hameed, Insights into the modeling of adsorption isotherm systems, Chem. Eng. J. 156 (2010) 2–10.

[34] J. Rouquerol, D. Avnir, C.W. Fairbridge, D.H. Everett, J.M. Haynes, N. Pernicone, J.D.F. Ramsay, K.S.W. Sing, K.K. Unger, Recommendations for the Characterization of porous solids, Pure Appl. Chem. 66 (1994) 1739 –1758.

[35] F.B. Cortés, F. Chejne, A rapid and novel approach for predicting water sorption isotherms and isosteric heats of different meat types, Meat Sci. 86 (2010) 921–925.

[36] N.N. Nassar, Asphaltene adsorption onto alumina nanoparticles: kinetics and thermodynamic studies, Energ. Fuel. 24 (2010) 4116–4122.

[37] N.N. Nassar, L.A. Arar, N.N. Marei, M.M. Abu Ghanim, M.S. Dwekat, S.H. Sawalha, Treatment of olive mill based wastewater by means of magnetic nanoparticles: Decolourization, dephenolization and COD removal, Environ. Nanotechnol. Monit. Manage. 1–2 (2014) 14–23.

[38] J.H. Huang, Molecular sieving effect of a novel hyper-cross-linked resin, Chem. Eng. J. 165 (2010) 265–272.

[39] J.H. Huang, X.F. Wu, H.W. Zha, B. Yuan, S.H. Deng, A hypercrosslinked poly(styrene-co-divinylbenzene) PS resin as a specific polymeric adsorbent for adsorption of 2-naphthol from aqueous solutions, Chem. Eng. J. 218 (2013) 267–275.

[40] X. Wu, Y. Liu, T. Huo, Z. Chen, Y. Liu, D. Di, M. Guo, L. Zhao, Multiple interactions on macroporous adsorption resins modified with ionic liquid, Colloid. Surfaces A: Physicochemical Eng. Aspects 487 (2015) 35–41.

[41] H.D. Qiu, A.K. Mallik, M. Takafuji, X. Liu, S.X. Jiang, H. Ihara, A new imidazolium-embedded C18 stationary phase with enhanced performance in reversed-phase liquid chromatography, Anal. Chim. Acta. 738 (2012) 95–101.

[42] W. Zheng, Y. Wang, L.Q. Yang, X.L. Li, L.C. Zhou, Y.F. Li, Novel adsorbent of polymeric complex derived from chaleting resin with Cu(II) and its removal properties for cyanide in aqueous solution, Colloid. Surfaces A: Physicochemical Eng. Aspects 455 (2014) 136–146.

Figure captions

Fig 1. Names, chemical structures and concentrations of phenolic compounds in OMW.

Fig. 2. ATR-FTIR spectra of (a) MN202 and (b) FPX66 after activation.

Fig. 3. Removal percentages of total phenols (a) and color (b) from OMW onto FPX66 and MN202.

Fig. 4. Adsorption isotherms of phenolic compounds onto FPX66 resin.

Fig. 5. Adsorption isotherms of phenolic compounds onto MN202 resin.

Fig 6. Desorption of the examined polyphenols from FPX66 (1) and MN202 (2) using ethanol (a) and 0.1M HCl in ethanol (b).

HD: Hydroxytyrosol, DA: 3,4 Dihydroxybenzoic acid, Ty: Tyrosol, Ca: Catechin, VA: Vanillic Acid, SA; Syringic Acid, CA: Caffeic Acid, Ph: Phenol, pCA: p-coumaric Acid.

Fig. 1

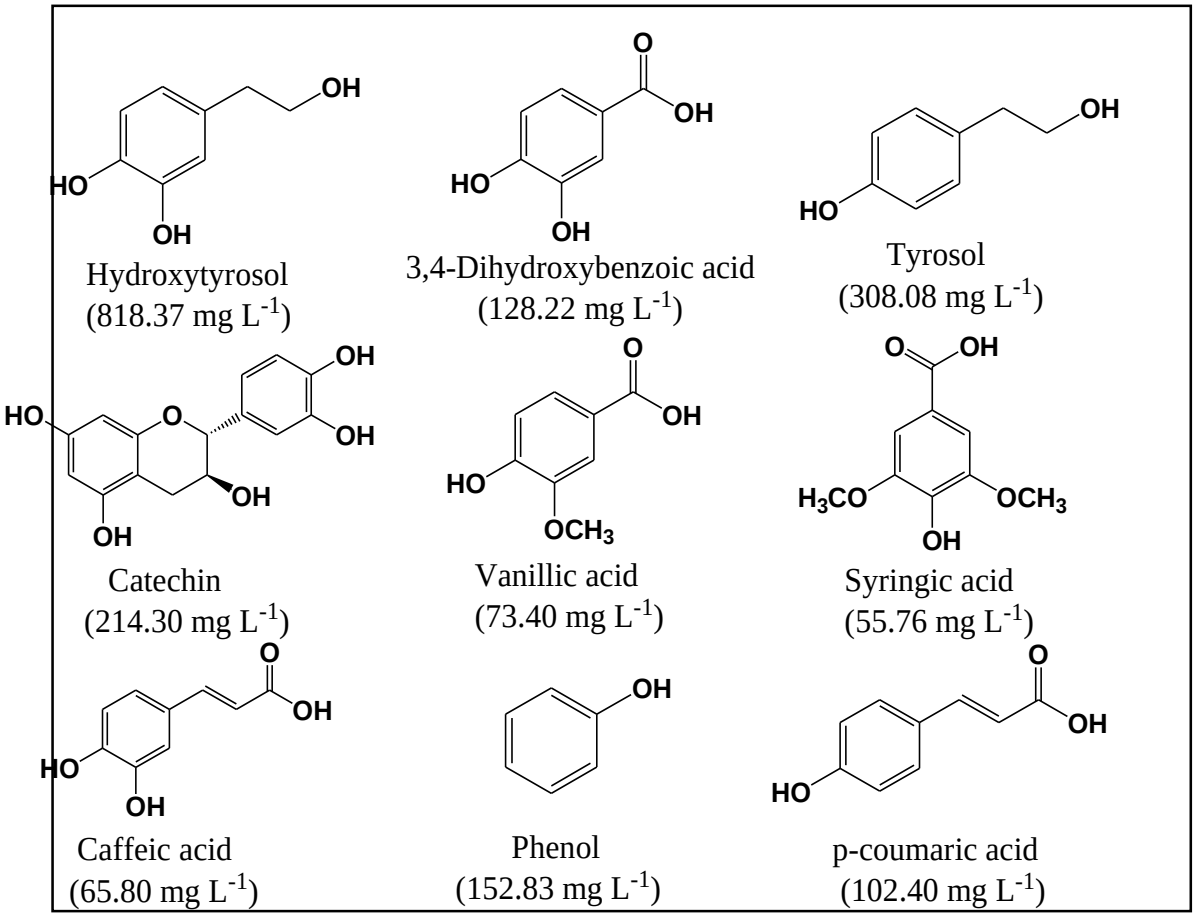

Fig. 2

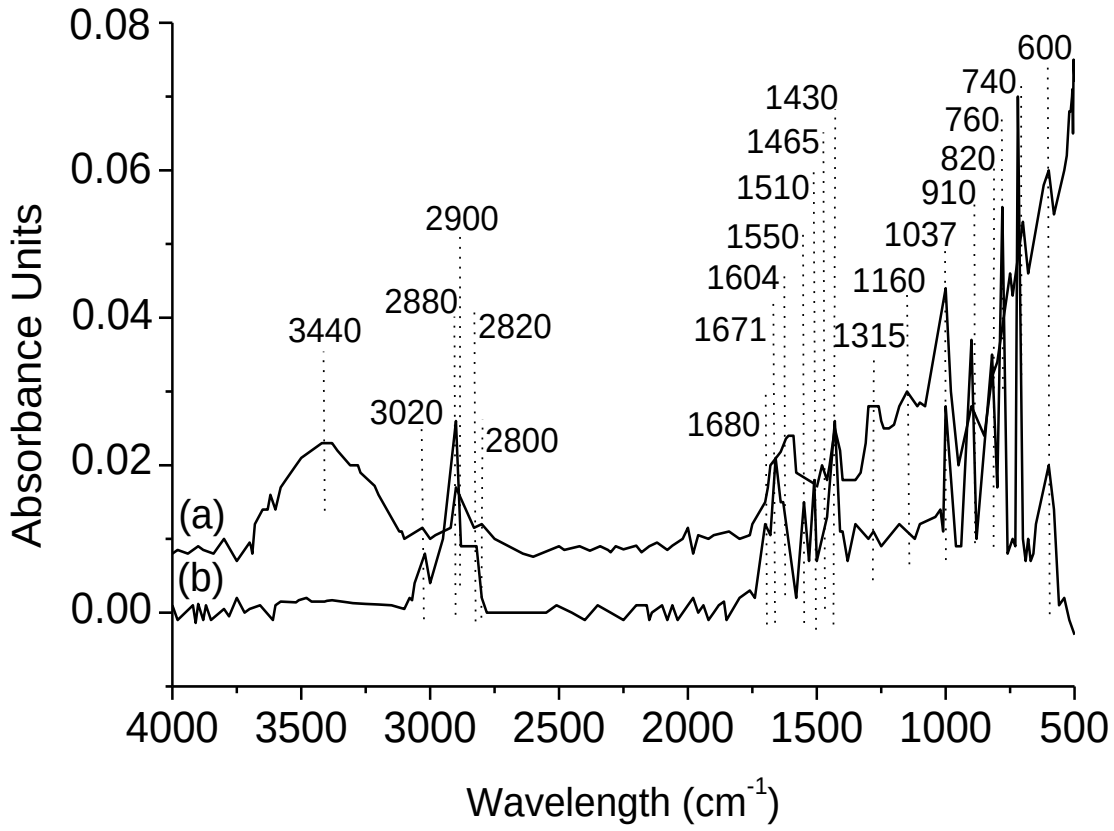

Fig. 3

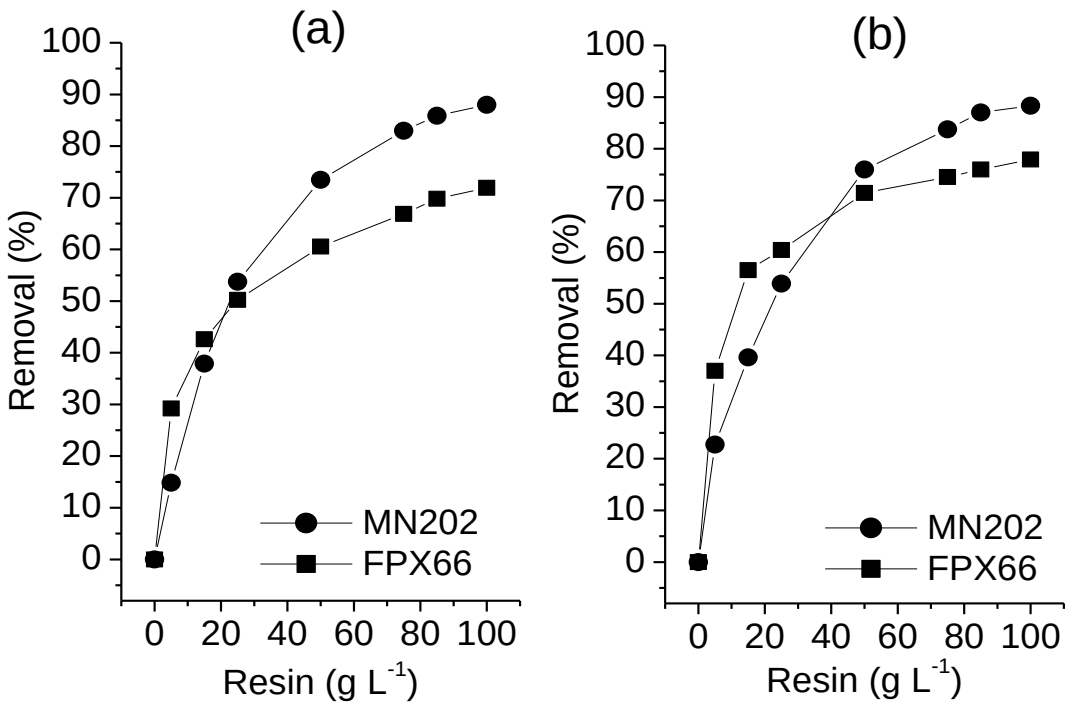

Fig. 4

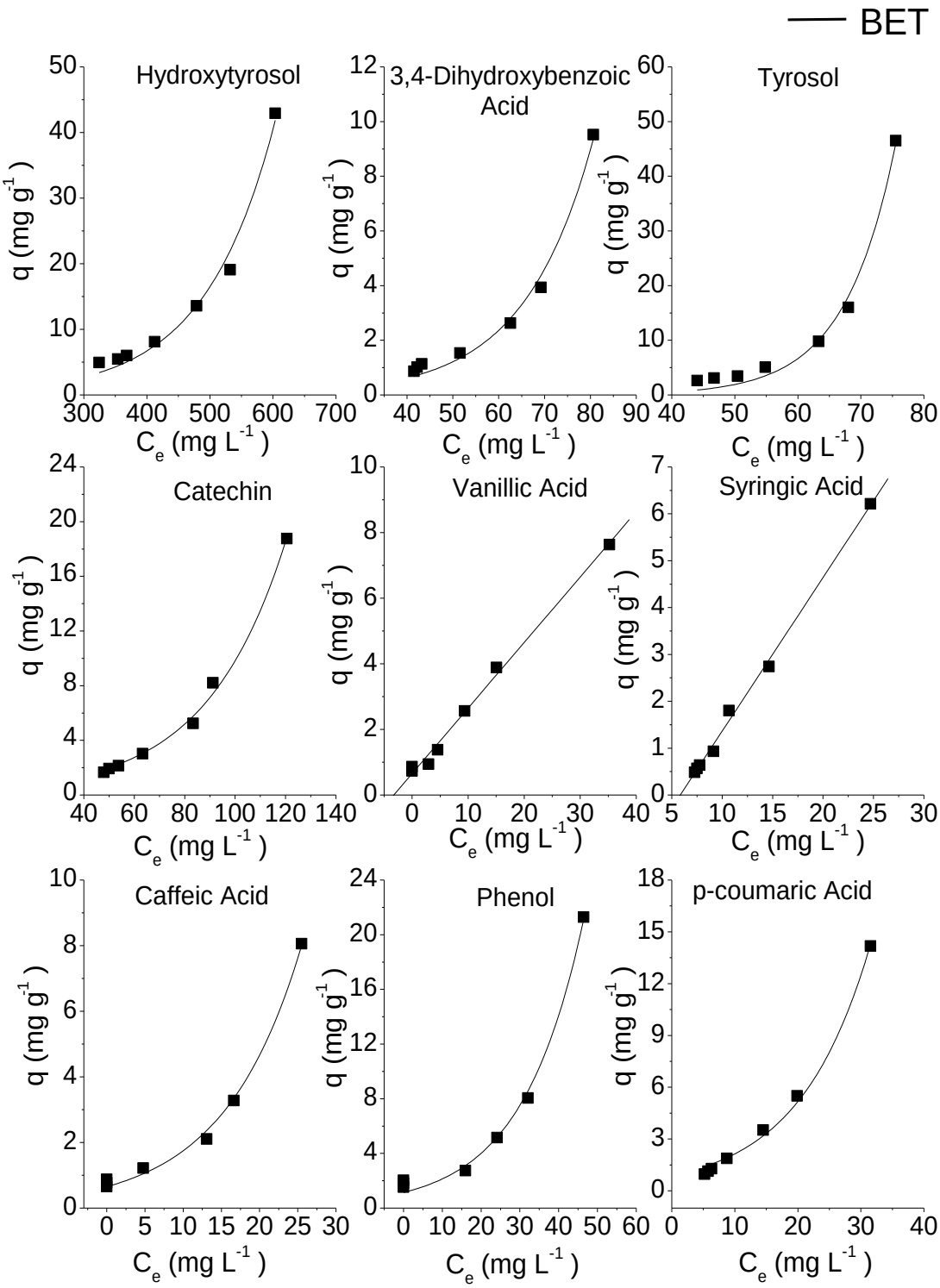

Fig. 5

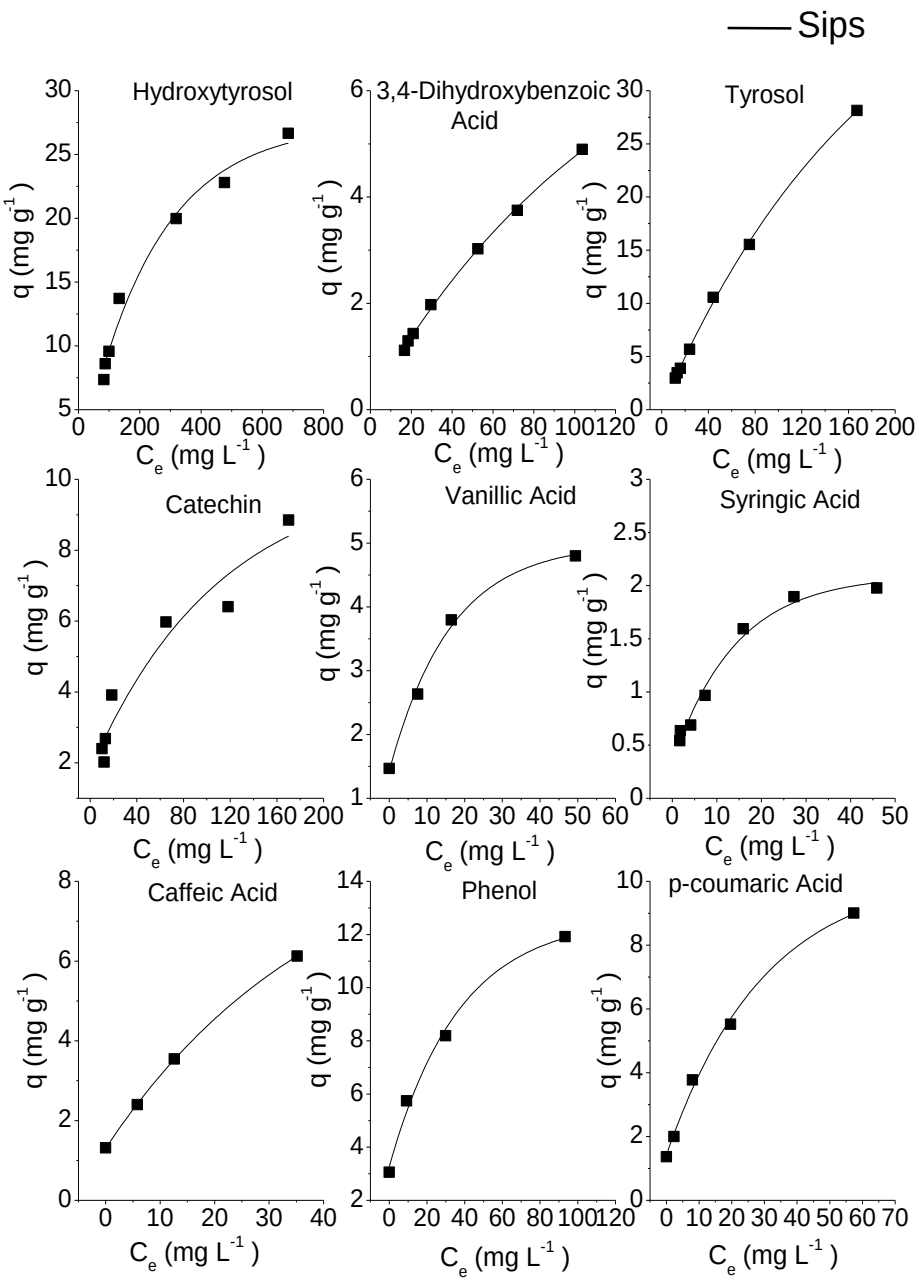

Fig. 6

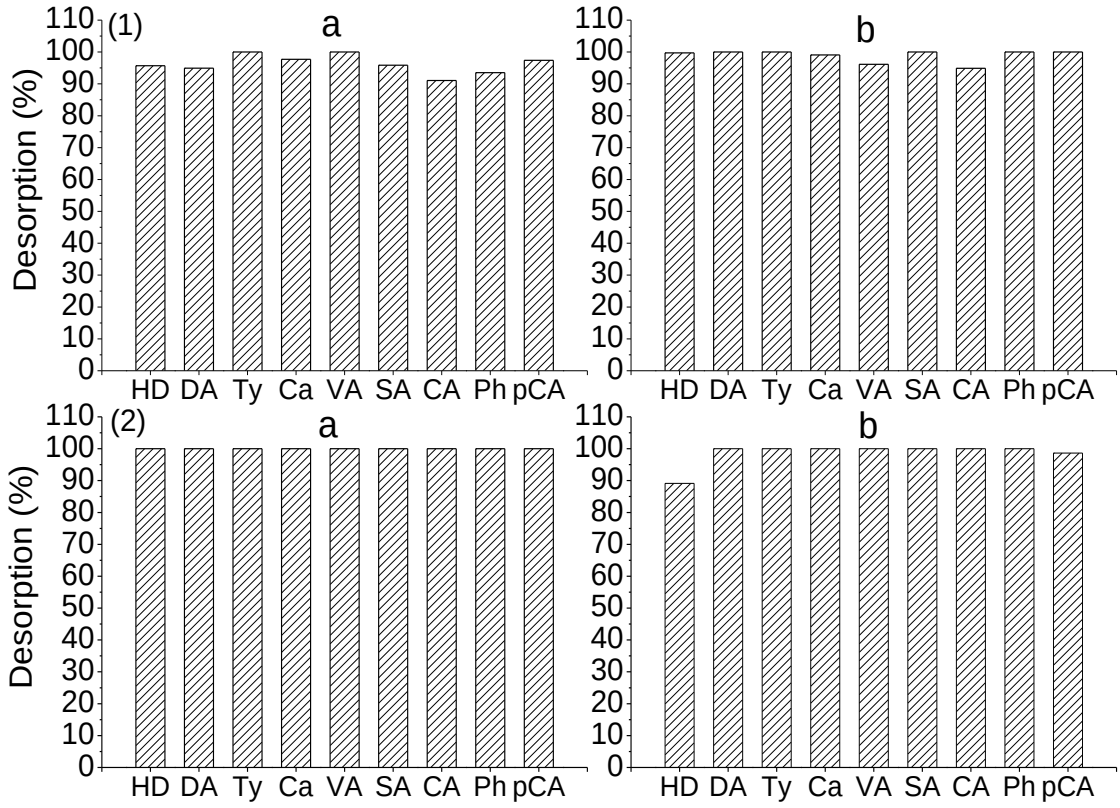

Table 1

Characteristics of OMW.

Parameters	Values
pH	4.4
COD (g L^{-1})	53.48
Total phenolic compounds (mg L^{-1})	3330

Table 2

Removal percentages (R_{Phenol} %) and selectivity coefficients (K) of phenolic compounds onto FPX66 and MN202.

Phenolic compounds	Resin (g L^{-1})	FPX66		MN202	
		R_{Phenol} (%)	K	R_{Phenol} (%)	K
Hydroxytyrosol	5	23.2	0.307	16.3	0.356
	50	49.4	0.601	84.8	0.920
3,4-Dihydroxybenzoic Acid	5	37.1	0.491	19.1	0.417
	50	59.8	0.727	76.9	0.834
Tyrosol	5	75.5	1.000	45.7	1.000
	50	82.2	1.000	92.2	1.000
Catechin	5	43.8	0.580	20.6	0.450
	50	70.4	0.857	91.3	0.990
Vanillic Acid	5	52.0	0.688	32.7	0.715
	50	93.8	1.141	100	1.084
Syringic Acid	5	55.7	0.738	17.7	0.387
	50	83.6	1.017	86.8	0.941
Caffeic Acid	5	61.2	0.810	46.6	1.019
	50	92.7	1.128	100	1.084
Phenol	5	74.6	0.988	40.0	0.875
	50	89.6	1.089	100	1.084
p-coumaric Acid	5	69.2	0.917	44.0	0.962
	50	91.5	1.112	97.7	1.059

Table 3

Best fitting of the experimental adsorption data of phenolic compounds onto FPX66.

Isotherm models	Hydroxytyrosol	3,4-Dihydroxybenzoic acid	Tyrosol	Catechin	Vanillic acid	Syringic acid	Caffeic acid	Phenol	*p*-coumaric acid
Langmuir									
q_m (mg g^{-1})	5.232	1.193	1.993	3.284	22.831	0.412	4.181	8.511	9.050
K_L (g L^{-1})	24.705	63.724	0.013	0.079	0.0140	0.076	0.026	0.899	0.019
R^2	0.991	0.994	0.987	0.964	0.968	0.969	0.991	0.995	0.990
ND	2.944	2.159	5.546	4.337	2.323	4.331	2.154	1.829	2.657
NSD	3.553	4.067	6.691	6.370	2.661	5.223	2.258	2.065	3.626
Freundlich									
K_F	1.12E-06	4.21E-05	3.78E-07	8.94E-05	0.370	9.32E-03	1.15E-02	1.33E-02	0.122
n	0.379	0.373	0.242	0.395	1.154	0.481	0.495	0.529	0.790
R^2	0.974	0.983	0.967	0.984	1	0.964	0.998	0.978	0.999
ND	7.336	6.918	9.915	7.318	1.346	7.938	1.821	7.227	1.921
NSD	8.470	8.241	11.612	7.243	2.152	10.447	1.966	8.471	4.008
Sips									
q_m(mg g^{-1})	4.103	0.940	1.492	3.404	53.009	0.354	8.376	8.702	8.732
K_s	0.39E-03	0.018	0.029	6.65E-3	6.83E-2	0.205	0.024	0.015	0.020
n	0.850	0.900	0.800	0.980	1.110	1.110	1.030	0.990	1.010
R^2	0.992	0.969	0.988	0.965	0.991	0.970	0.993	0.995	0.989
ND	3.348	3.426	3.782	2.893	0.408	3.475	1.890	1.862	1.778
NSD	4.140	5.025	4.343	4.696	0.493	5.412	2.891	2.089	3.512
Redlich-Peterson									
K_{RP} (L g^{-1})	1.60	1	3	8	1	0.28	1	5	4

a_{RP}	6.04E06	5.65E03	1.29E07	9.44E04	1.673	5.75E02	4.032	4.24E02	3.20E01
β	1.878	1.372	3.259	1.544	0.210	2.675	1.334	0.945	0.281
R^2	0.960	0.944	0.942	0.957	0.991	0.972	0.991	0.903	0.978
ND	4.720	10.145	9.876	4.376	1.063	5.705	2.480	8.879	1.935
NSD	6.454	11.079	10.839	5.229	1.281	7.916	2.704	9.123	3.058
BET									
K_L (L mg^{-1})	6.86E-02	1.01E-03	1.98E-03	E-03	9.70E-03	6.40E-03	4.40E-02	E-03	1.20E-03
K_S (L mg^{-1})	6.68E-02	0.117	1.08E-02	7.05E-03	4.99E-02	0.71E-02	1.662	1.41E-02	1.76E-02
q_m (mg g^{-1})	2.103	9.136	2.167	2.955	6.931	0.405	0.872	9.138	9.872
R^2	0.980	0.986	0.987	0.971	0.998	0.965	0.999	0.994	0.989
ND	1.376	1.334	1.155	2.549	1.065	2.542	0.455	1.671	1.241
NSD	1.482	1.784	1.633	3.867	0.895	3.801	0.470	2.143	1.765

Table 4

Best fitting of the experimental adsorption data of phenolic compounds onto MN202.

Isotherm models	Hydroxytyrosol	3,4-Dihydroxybenzoic acid	Tyrosol	Catechin	Vanillic acid	Syringic acid	Caffeic acid	Phenol	*p*-coumaric acid
Langmuir									
q_m (mg g^{-1})	40.650	12.515	77.519	9.891	5.605	2.302	9.183	12.578	11.062
K_L (g L^{-1})	3.16E-03	6.10E-03	3.40E-03	0.026	0.237	0.138	0.056	0.124	0.068
R^2	0.980	0.982	0.976	0.951	0.999	0.984	0.986	0.973	0.976
ND	3.242	1.824	1.835	10.794	1.152	1.733	4.669	2.856	6.621
NSD	5.894	2.138	2.542	11.676	1.366	2.357	5.391	3.156	9.226
Freundlich									
K_F	0.687	0.127	0.375	0.812	1.465	0.385	0.954	2.835	1
n	1.749	1.260	1.168	2.174	3.20	2.165	1.917	3.169	1
R^2	0.952	0.996	0.996	0.932	0.951	0.944	0.999	0.999	1
ND	4.001	2.787	3.837	3.096	5.068	6.068	0.529	0.707	8.842
NSD	4.509	3.500	4.791	3.746	5.349	8.339	0.564	0.754	9.684
Sips									
q_m(mg g^{-1})	32.444	10.759	59.270	8.717	4.880	2.003	6.579	12.255	10.94
K_s	1.65E-3	6.22E-03	3.69E-03	1.04E-05	0.032	0.029	0.011	0.004	0.068
n	0.83	095	0.93	0.33	0.53	0.50	0.50	0.50	0.98
R^2	0.993	0.987	0.985	0.985	0.999	0.999	0.996	0.998	0.978
ND	1.600	1.543	2.864	1.689	0.216	0.637	0.296	0.184	4.885
NSD	2.213	1.754	0.469	1.689	0.153	0.715	0.896	0.788	6.031
Redlich-Peterson									
K_{RP} (L g^{-1})	1	1	7	14	1	2	1	2	2
a_{RP}	0.876	6.410	705.401	16.792	0.317	3.703	0.453	0.369	0.774

β	0.503	0.243	0.552	0.544	0.859	0.636	0.664	0.817	0.679
R^2	0.953	0.977	0.997	0.950	0.996	0.980	0.996	0.997	0.998
ND	9.337	3.547	2.939	2.119	2.138	1.089	1.521	2.286	2.335
NSD	11.649	4.077	3.939	3.970	2.996	1.328	2.239	3.470	2.583